Asian Journal of Chemistry; Vol. 36, No. 10 (2024), 2329-2336

ASIAN JOURNAL OF CHEMISTRY

https://doi.org/10.14233/ajchem.2024.32337

Fabrication of Silica Gel Reinforced, Cadmium Oxalate based Extrinsic Crystalline Materials and their Characterization

A.S. GANAVI[1], N. JAGANNATHA[1,*], K.P. NAGARAJA[2], DELMA D'SOUZA[2] and P.S. ROHITH[2]

[1]Department of Physics, University College Mangalore (A Constituent College of Mangalore University), Mangalore-575001, India
[2]Department of Physics, Field Marshal K.M. Cariappa College, Madikeri-571201, India

*Corresponding author: E-mail: jagannathnettar64@gmail.com

Received: 19 July 2024; *Accepted*: 26 August 2024; *Published online*: 30 September 2024; AJC-21764

Cobalt-lead mixed cadmium oxalate (CoLMCO) and zinc-lead mixed cadmium oxalate (ZnLMCO) extrinsic crystalline materials were grown in oxalic acid embedded silica hydrogel. In an optimized gel environment, the extrinsic Co^{2+}-Pb^{2+} and Zn^{2+}-Pb^{2+} combinations fit well in the parental Cd^{2+} vacancies and emerged as distinct CoLMCO and ZnLMCO novel materials. The inherent properties of CoLMCO and ZnLMCO crystals were characterized by analytical and spectroscopic methods. Energy dispersive X-ray (EDX) analysis attached with field emission scanning electron microscope (FESEM) was employed to identify the chemical composition and morphology of the crystals. Fourier transform infrared (FTIR) spectral analysis confirmed the presence of oxalate group, water of crystallization and metal-oxygen bonds in the crystals. Thermal studies confirmed two phases of decomposition and ensured stability up to 1112.78 ºC for CoLMCO crystals and 1071.65 ºC for ZnLMCO crystals in a metal-oxide state. Bragg's diffraction patterns revealed the high crystallinity of the materials and observed triclinic geometry in them. The UV-visible spectral studies of CoLMCO and ZnLMCO crystals showed maximum transparency to visible light and absorption in the UV region, possessing absorption maximum A_{max} = 1.588 and 1.276; optical band gap energies E_g = 5.638 eV and 5.845 eV, respectively. The V-I characteristics of the prepared crystals unveiled a feeble current flow (nA), exhibiting linear variation with applied DC voltage (0-200 V) leading leakage resistances of 1.187 GΩ (CoLMCO) and 5.176 GΩ (ZnLMCO). Dielectric constants of mixed crystals varied inversely with applied frequency and became almost stable at the mid-radio frequency range.

Keywords: Band gap energy, Crystals, Dielectric constant, Oxalate.

INTRODUCTION

Novel and high-quality crystalline materials with unique physical and opto-electrical properties are essential for today's technological applications. Transition metal ions exhibit various coordination numbers and geometries in complex forms. This adaptability arises from their ability to accommodate distinct ligands around the metal core. The divalent metallic complexes gather special interest due to their very good coordination geometry with oxalates [1-4]. Oxalate crystals of various metallic complexes exhibit very high thermal stability in the metal oxide states [5,6]. In present investigation, among the transition metals, cobalt and zinc are taken with lead and cadmium to form complexes during the growth of mixed oxalate crystals. The heavy element lead is formed in high abundance as the end product during the radioactive decay of elements in cosmic events [7].

Lead is the major constituent in lead-acid batteries whereas cadmium in nickel-cadmium batteries [8,9]. Cobalt is used in electroplating due to its attractive appearance, hardness and resistance to corrosion. Cobalt in lithium-ion batteries as $LiCoO_2$ cathode, offers high conductivity and structural stability during charge cycling [10,11]. Zinc is used in electrical and automobile industries due to its galvanizing and die-casting applications [12]. Thus, cobalt-lead mixed cadmium oxalate (CoLMCO) and zinc-lead mixed cadmium oxalate (ZnLMCO) crystalline materials were fabricated in purest form using gel crystal growth technique; their chemical constituents and opto-electrical-dielectric parameters were analyzed.

EXPERIMENTAL

Growth of CoLMCO and ZnLMCO crystals: The fabrication of cobalt-lead mixed cadmium oxalate (CoLMCO)

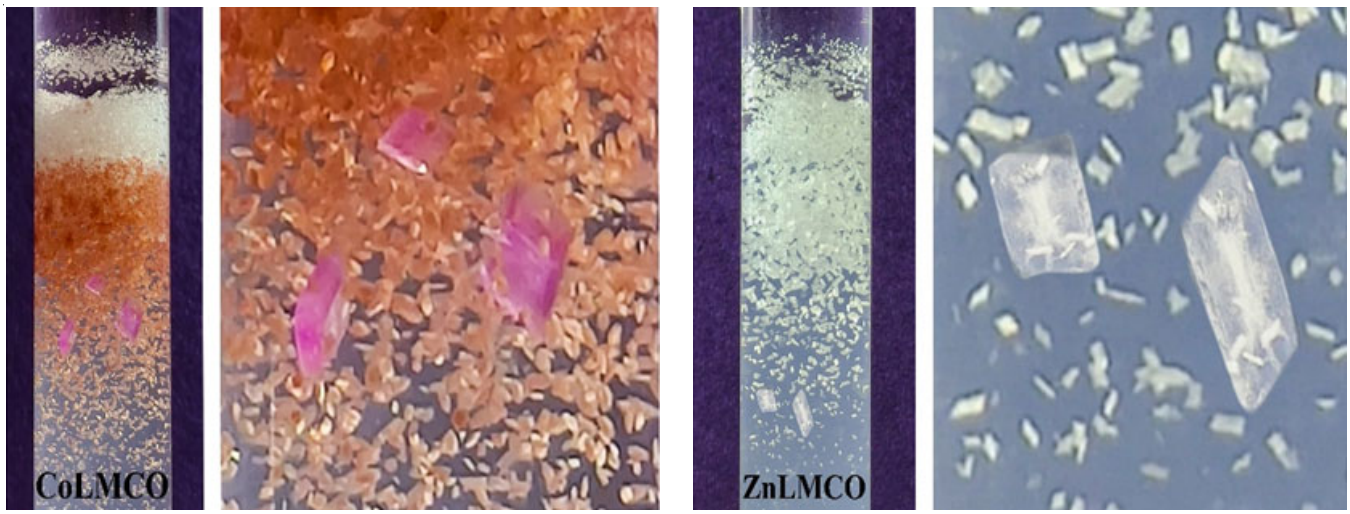

Fig. 1. Growth of crystals in oxalic acid embedded silica (OES) gel

and zinc-lead mixed cadmium oxalate (ZnLMCO) crystalline materials was accomplished by gel technique with oxalic acid reinforced silica hydrogel as growth media. Oxalic acid embedded silica (OES) hydrogel was prepared by mixing sodium metasilicate (SMS) solution of specific gravity 1.0375 g cm^{-3} and oxalic acid of concentration 0.5 M in 5:4 ratio and allowed to set for gelling (gel pH = 4.2) [13,14]. To the set gel (gel sets in 5 days at 26 ºC), the solution of nitrates of Cd^{2+}:Pb^{2+}:Co^{2+} cations in the ratio 1:1:1 were added to form CoLMCO crystals; zinc nitrate, lead nitrate and cadmium nitrate mixture in the ratio 1:1:1 as a supernatant solution to fabricate ZnLMCO crystals. At an optimized growth environment (Table-1) diffusion of the cations into nucleation sites began, the growth established and advanced for up to 15 days (CoLMCO) and 10 days (ZnLMCO) (Fig. 1). After growth saturation, CoLMCO and ZnLMCO crystals were extracted from the gel (Fig. 2) and were found hard, transparent, water-insoluble and corrosion resistant.

The chemical process describing the growth of CoLMCO and ZnLMCO crystalline materials as follows:

$$Co^{2+} + Pb^{2+} + Cd(NO_3)_2{\cdot}4H_2O + C_2H_2O_4{\cdot}2H_2O \longrightarrow Cd{:}Pb{:}Co(C_2O_4){\cdot}3H_2O + 2HNO_3 + 3H_2O$$

$$Zn^{2+} + Pb^{2+} + Cd(NO_3)_2{\cdot}4H_2O + C_2H_2O_4{\cdot}2H_2O \longrightarrow Cd{:}Pb{:}Zn(C_2O_4){\cdot}3H_2O + 2HNO_3 + 3H_2O$$

Characterization: After the extraction, the CoLMCO and ZnLMCO crystals were subjected to analytical, optical and electrical characterizations to determine their inherent properties. CARL ZEISS FESEM attached EDS system measured the chemical constituents and cationic distribution present in the prepared crystals. The Thermo-Nicolet iS50 FTIR spectrometer was used to identify various bonds that form the skeleton of the crystals. TGA-DTA (Hitachi STA 7300) was utilized to study the thermal behaviour of CoLMCO and ZnLMCO crystals from room temperature to 1300 ºC. Utilizing the Bruker D8 Advance A25 diffractometer, the Bragg's diffraction patterns of crystalline materials were found. The crystal transparencies to UV-visible light were studied using a UV-VIS-NIR θ/2θ spectrophotometer (HO-SPA-1990P). The V-I characteristic of embedded crystals was explored by two probe method and the dielectric measurements were done with Agilent 4294A Precision Impedance Analyzer.

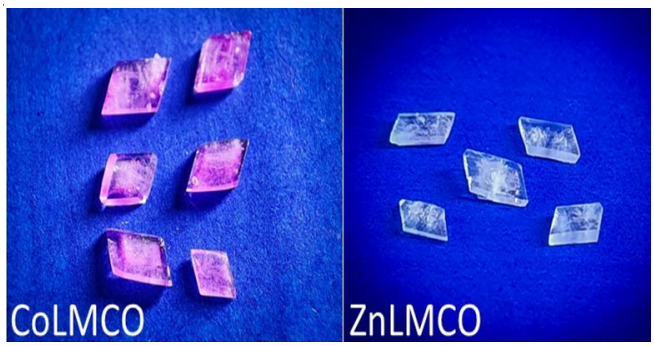

Fig. 2. Extracted CoLMCO and ZnLMCO crystals

TABLE-1
OPTIMAL GROWTH CONDITIONS OF OXALATE CRYSTALS

Growth parameters	CoLMCO	ZnLMCO
Specific gravity of SMS solution	1.0375 g cm^{-3}	1.0375 g cm^{-3}
Concentration of oxalic acid	0.5 M	0.5 M
SMS:Oxalic acid	5:4	5:4
Gel pH	4.2	4.2
Concentration of cobalt nitrate, zinc nitrate, lead nitrate and cadmium nitrate	0.5 M	0.5 M
Ratio of cationic reactants	1:1:1	1:1:1
Crystal growth period	15 days	10 days
Physical appearance	Pink transparent	Colourless transparent
Size (l × b × h)	3.23 × 2.80 × 1.30 mm^3	2.76 × 2.15 × 0.89 mm^3

RESULTS AND DISCUSSION

EDX-FESEM measurements: The presence of respective elements in the prepared crystals (CoLMCO and ZnLMCO) were identified in the characteristic peaks of respective energy dispersive X-ray spectrums (Fig. 3) [15,16]. Various elements and their corresponding quantities present in the crystal formation are shown in Table-2. CoLMCO crystal ingrains a cationic distribution of Cd^{2+}:Pb^{2+}:Co^{2+} = 245:4:1, whereas in ZnLMCO it is about Cd^{2+}:Pb^{2+}:Zn^{2+} = 59.25:2.25:1. Cationic distributions measured using EDX analysis were in contrast to the cationic mixture at growth phase (Cd^{2+}:Pb^{2+}:Co^{2+} = Cd^{2+}: Pb^{2+}:Zn^{2+} = 1:1:1). In CoLMCO and ZnLMCO embedded crystals, Cd^{2+} ions predominate over Pb^{2+}, Co^{2+} and Zn^{2+} ions, proposed as the primary cation in the emphasized crystals. The vacancies of Cd^{2+} ions occupied by extrinsic Pb^{2+} ions and Co^{2+} ions are in the ratio Pb^{2+}:Co^{2+} = 4:1 in CoLMCO and in ZnLMCO the occupation of extrinsic Pb^{2+} ions and Zn^{2+} ions is in the ratio Pb^{2+}:Zn^{2+} = 2.25:1. Both in CoLMCO and ZnLMCO crystals the diffusion of Cd^{2+} ions and movements of $C_2O_4^{2-}$ ions into the nucleation sites balanced well compared to $C_2O_4^{2-}$ ion interaction with other cations (Pb^{2+}, Co^{2+} and Zn^{2+}). Thus, Cd^{2+} cations form stable bonds with $C_2O_4^{2-}$ ions and originated as a perfect crystal in gel technique; whereas other extrinsic cations in the mixture (Pb^{2+}, Co^{2+} and Zn^{2+}) behave as dopant ions and occupy only the parent Cd^{2+} vacancies and formed as stable mixed oxalate crystals.

TABLE-2
CHEMICAL COMPOSITION OF
CoLMCO AND ZnLMCO CRYSTALS

Elements	CoLMCO		ZnLMCO	
	Weight (%)	Atomic (%)	Weight (%)	Atomic (%)
Cd	15.87	2.42	37.17	7.46
Pb	0.47	0.04	2.56	0.28
Co	0.08	0.01	–	–
Zn	–	–	0.38	0.13
O	60.77	65.02	43.53	61.42
C	22.81	32.51	16.36	30.71
Total	100	100	100	100

The FESEM images of the CoLMCO and ZnLMCO crystals at 5 kV with a resolution of 100 µm (Fig. 4) revealed the aggregates of unusual geometries in layered formations.

FTIR spectral studies: The functional groups such as oxalate, water of crystallization and metal-oxygen (M-O) bonds in CoLMCO and ZnLMCO crystals were identified by FTIR spectrum (Fig. 5) with the wavenumber ranging from 4000 to 400 cm^{-1} and the band assignments are listed in Table-3 [17,18]. The absorption peaks corresponding to symmetric and asymmetric stretching of the O-H group and water of crystallization indicate the presence of coordinated water molecules. The absorption bands attributed to C=O stretching, O-H bending, C-C vibrations, C-O stretching, O-H out of plane bending, M-O bonding and M-O stretching confirmed the presence of oxalate group and M-O linkages in both crystals. The shift in the absor-

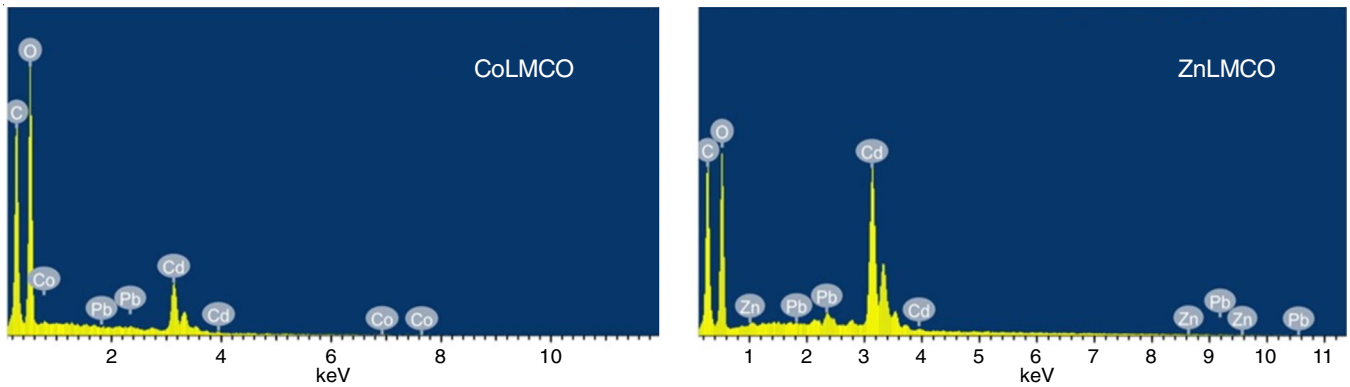

Fig. 3. EDX spectra of CoLMCO and ZnLMCO crystals

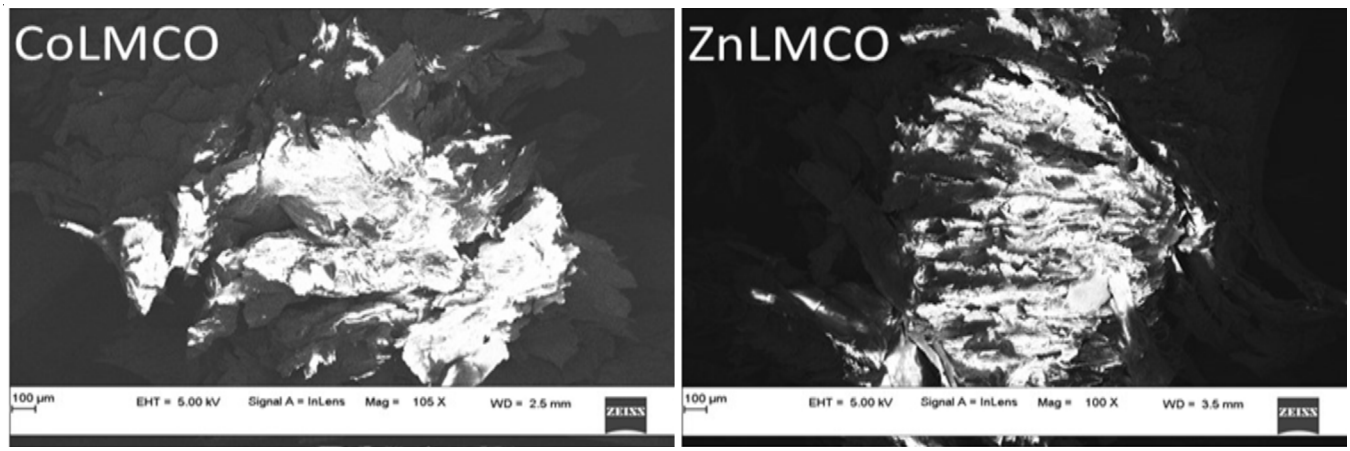

Fig. 4. FESEM images of CoLMCO and ZnLMCO crystals

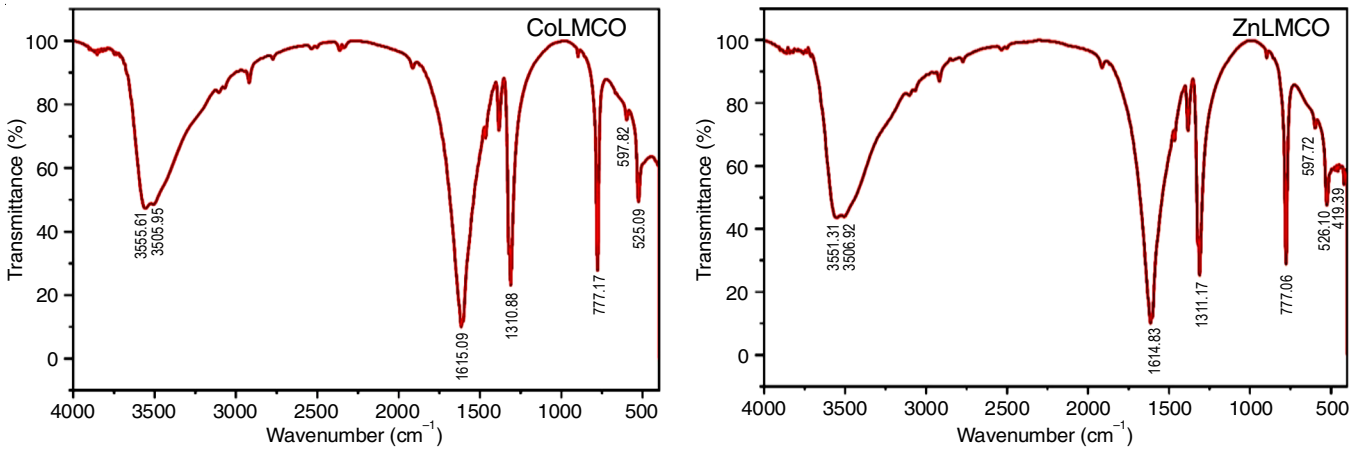

Fig. 5. FTIR spectrum of CoLMCO and ZnLMCO crystals

TABLE-3
FTIR BAND ASSIGNMENTS OF CoLMCO AND ZnLMCO CRYSTALS

Band assignments	Wavenumbers (cm^{-1})	
	CoLMCO	ZnLMCO
Symmetric and asymmetric stretching of OH group and water of crystallization	3555.61, 3505.95	3551.31, 3506.92
C=O stretching, O-H bending	1615.09	1614.83
C-C vibrations, C-O stretching	1310.88	1311.17
O-H out of plane bending, M-O bonding	777.17	777.06
M-O stretching	597.82, 525.99	597.72, 526.10, 419.39

ption spectra and variation in fingerprint region specifies the distinctness among the CoLMCO and ZnLMCO crystals.

Thermal studies: Thermogravimetric analysis (TGA), derivative thermogravimetry (DTG) and differential scanning calorimetry (DSC) were employed to study the decomposition behaviour of CoLMCO and ZnLMCO crystals from room temperature to 1300 ºC [19,20]. Fig. 6 consists of TGA, DTG and DSC, show two phases of decomposition exhibited by the mixed crystals. The dehydration of crystal was accomplished at the temperature range T_D = 77.39 to 198.62 ºC (WL_o = 20.85%, T_{DTG} = 156 ºC and T_{DSC} = 167 ºC) for CoLMCO. The ZnLMCO crystal exhibits the first phase of decomposition for the T_D range 71.38-175.94 ºC (WL_o = 21.32 %, T_{DTG} = 139 ºC and T_{DSC} = 149 ºC). The second phase of degradation of CoLMCO crystal occurs at T_D range 273.71-363.90 ºC (WL_o = 27.36%, T_{DTG} = 333 ºC and T_{DSC} = 351 ºC); whereas anhydrous ZnLMCO crystal degrades at T_D = 284.56 to 391.80 ºC (WL_o = 28.04%, T_{DTG} = 349 ºC and T_{DSC} = 358 ºC) both loosing carbon monoxide and carbon dioxide simultaneously. Thereafter, both crystals remained stable in the metal oxide state for temperatures above 1000 ºC (CoLMCO existed in Cd:Pb:Co-O state until 1112.78 ºC and ZnLMCO in Cd:Pb:Zn-O up to 1071.65 ºC), which were evident from DTG and DSC curves. Tables 4 and 5 elucidates the results of thermal studies. The observed weight loss % (WL_o) was in close agreement with theoretically estimated weight loss % (WL_c). TGA and FTIR spectral analysis confirm the presence of crystalline water which accumulates as debris in the crystal formation of both CoLMCO and ZnLMCO crystalline materials. Overall, the CoLMCO crystal ingrained with a chemical formula $Cd_{0.980}Pb_{0.016}Co_{0.004}(C_2O_4)\cdot 3H_2O$ with a formula weight of 255.78, whereas ZnLMCO suggested with a molecular formula of $Cd_{0.948}Pb_{0.036}Zn_{0.016}(C_2O_4)\cdot 3H_2O$ (m.w. = 257.13).

Powder XRD studies: Powder X-ray diffraction (PXRD) measurements confirmed the high crystallinity of CoLMCO

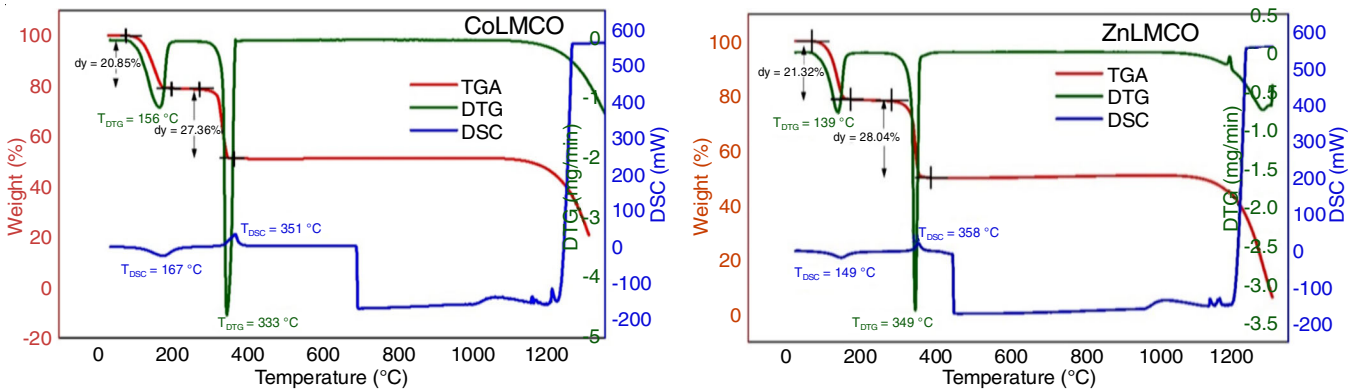

Fig. 6. Degradation behaviour of CoLMCO and ZnLMCO crystals

TABLE-4
THERMAL STUDIES PROFILE OF CoLMCO AND ZnLMCO CRYSTALS

Crystals	Phase	Decomposition temperature, T_D (°C)	T_{DTG} (°C)	T_{DSC} (°C)	Weight loss (%)		m.w.
					Observed WL_o	Calculated WL_c	
CoLMCO	I	77.39-198.62	156	167	20.85	21.13	255.78
	II	273.71-363.90	333	351	27.36	28.16	
ZnLMCO	I	71.38-175.94	139	149	21.32	21.02	257.13
	II	284.56-391.80	349	358	28.04	28.01	

TABLE-5
CHEMICAL PROCESS FOLLOWED BY THE CRYSTALS IN THEIR DEGRADATION

Crystals	Phase	Degradation process
CoLMCO	I	$(Cd_{0.980}Pb_{0.016}Co_{0.004})C_2O_4{\cdot}3H_2O \longrightarrow (Cd_{0.980}\,Pb_{0.016}\,Co_{0.004})\,C_2O_4 + 3H_2O$
	II	$(Cd_{0.980}Pb_{0.016}Co_{0.004})C_2O_4 \longrightarrow (Cd_{0.980}Pb_{0.016}Co_{0.004})O + CO + CO_2$
ZnLMCO	I	$(Cd_{0.948}Pb_{0.036}Zn_{0.016})C_2O_4{\cdot}3H_2O \longrightarrow (Cd_{0.948}Pb_{0.036}Zn_{0.016})C_2O_4 + 3H_2O$
	II	$(Cd_{0.948}Pb_{0.036}Zn_{0.016})C_2O_4 \longrightarrow (Cd_{0.948}Pb_{0.036}Zn_{0.016})\,O + CO + CO_2$

and ZnLMCO compounds (Fig. 7). To identify the exact crystalline nature, the diffraction patterns of the materials were indexed using N-treor-09 program and refined with CHEKCELL software [21,22]. The lattice parameters of both CoLMCO and ZnLMCO crystals (Table-6) exhibited triclinic geometry with space group *P*1.

TABLE-6
UNIT CELL PARAMETERS –
CoLMCO AND ZnLMCO CRYSTALS

Cell parameters	CoLMCO	ZnLMCO
a (Å)	5.994	5.992
b (Å)	6.653	6.612
c (Å)	8.485	8.460
α (°)	74.52	74.42
β (°)	74.15	74.61
γ (°)	80.82	81.17
Volume (Å^3)	312.323	310.018
Space group	*P*1	*P*1
Geometry	Triclinic	Triclinic

The cumulative results of EDX, FTIR and TG analysis confirmed the cationic matrix of Cd^{2+}:Pb^{2+}:Co^{2+} and Cd^{2+}:Pb^{2+}:Zn^{2+}; nucleation of them with $C_2O_4^{2-}$ ions formed the stable CoLMCO and ZnLMCO crystals. The crystalline materials showed extremely high thermal stability in the Cd:Pb:Co-O (1112.78 ºC) and Cd:Pb:Zn-O (1071.65 ºC) states. The embedded crystals with exceptional thermal stability (in oxide state) and high crystallinity encompass a variety of applications, duly in high temperature and microelectronics.

Opto-electrical studies: Optical and electrical properties of crystalline materials were unveiled using UV-visible spectroscopy, V-I characteristics and dielectric studies. Both CoLMCO and ZnLMCO crystals showed narrow absorbance in the UV region (Fig. 8) with an absorption maximum at λ = 205 nm (A_{max} = 1.588) and λ = 199.5 nm (A_{max} = 1.276) sequentially. In the wavelength range of 300-900 nm, the crystals exhibited a wide transparency window. The Tauc plot (Fig. 8) measured the optical band gap energy E_g = 5.638 eV (CoLMCO) and E_g = 5.845 eV (ZnLMCO) which prevailed the crystals as the insulators. Further, refractive index (n), reflectance (R) and electrical susceptibility (χ_e) were calculated (Table-7) using the following relations [23-25]:

$$E_g e^n = 36.3\,, \qquad R = \left(\frac{n-1}{n+1}\right)^2, \qquad \chi_e = n^2 - 1$$

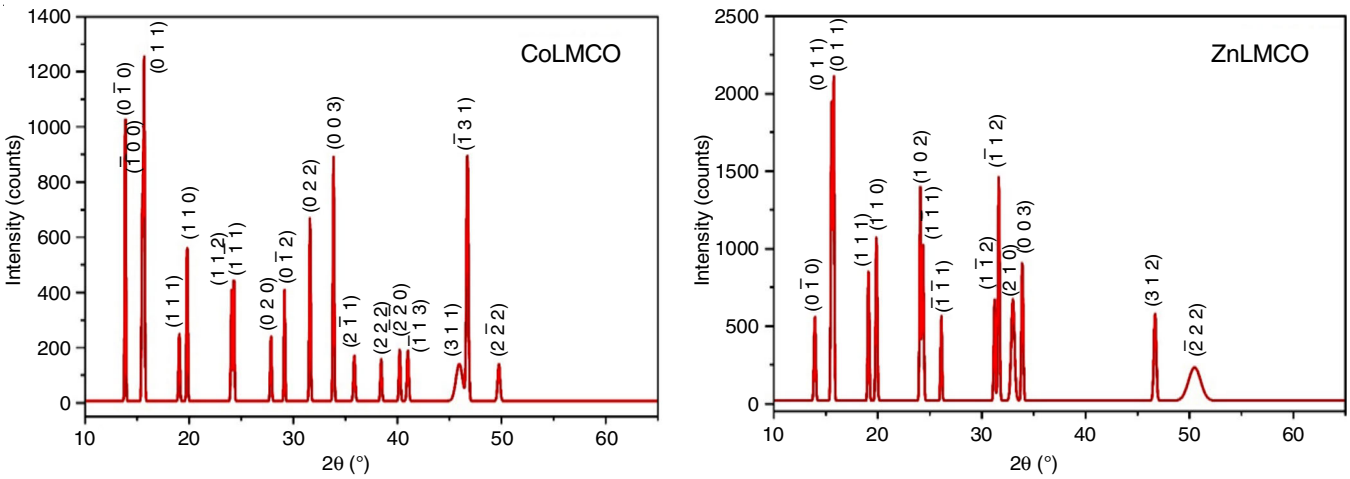

Fig. 7. PXRD spectrum of CoLMCO and ZnLMCO crystals

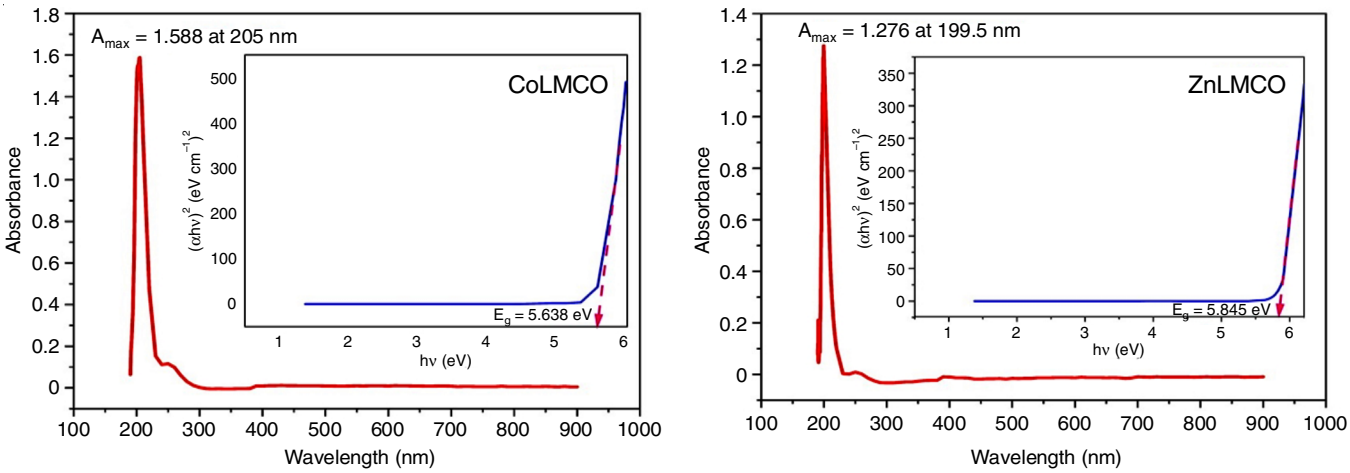

Fig. 8. UV-visible spectrum of CoLMCO and ZnLMCO crystals

TABLE-7
OPTO-ELECTRICAL PARAMETERS OF CoLMCO AND ZnLMCO CRYSTALS

Crystal	Band gap energy, E_g (eV)	Refractive index (n)	Reflectance (R)	Electrical susceptibility (χ_e)	Leakage resistance, R_L (GΩ)	Electrical resistivity, ρ (Ω m)	Electrical conductivity, σ (S m^{-1})
CoLMCO	5.638	1.862	0.091	2.467	1.187	15.747×10^7	6.350×10^{-9}
ZnLMCO	5.845	1.826	0.085	2.334	5.176	68.667×10^7	1.456×10^{-9}

Comparatively, the higher E_g value of ZnLMCO crystal reduced the refractive index (n = 1.826) in turn reflectance (R = 0.085) and electrical susceptibility (χ_e = 2.334). Further, the electrical behaviour of embedded crystals were analyzed by the variation of current for applied DC voltage [26] using two probe method (Fig. 9) and reported in Table-7. The CoLMCO crystal with lower band gap energy possessed leakage resistance of R_L= 1.187 GΩ, electrical resistivity ρ = 15.747×10^7 Ω m and DC conductivity σ = 6.350×10^{-9} S m^{-1} while the ZnLMCO crystal dominated over CoLMCO with R_L= 5.176 GΩ and ρ = 68.667×10^7 Ω m (σ = 1.456×10^{-9} S m^{-1}).

The dielectric behaviour of CoLMCO and ZnLMCO crystals was studied as a function of frequency. Both the crystalline materials exhibited linear decay of dielectric constant (Fig. 10) and dielectric loss (Fig. 11) with applied frequency up to 25 kHz and thereafter almost stable state was observed at megahertz. The reduced dielectric constant and dielectric loss at higher frequencies indicate improved optical efficiency and its implementation as optoelectronics devices [27,28].

The AC conductivity (Fig. 12) of embedded crystals increased at the initial phase and a sudden decrease in its conductance indicates the resonance behaviour in both CoLMCO and ZnLMCO crystals. The maximum conductance of $\sigma_{AC(max)}$ = 1.744×10^{-4} S m^{-1} at frequency f_r = 2.125 MHz in CoLMCO and $\sigma_{AC(max)} = 3.157 \times 10^{-5}$ S m^{-1} at frequency f_r = 2.175 MHz in ZnLMCO crystals were observed.

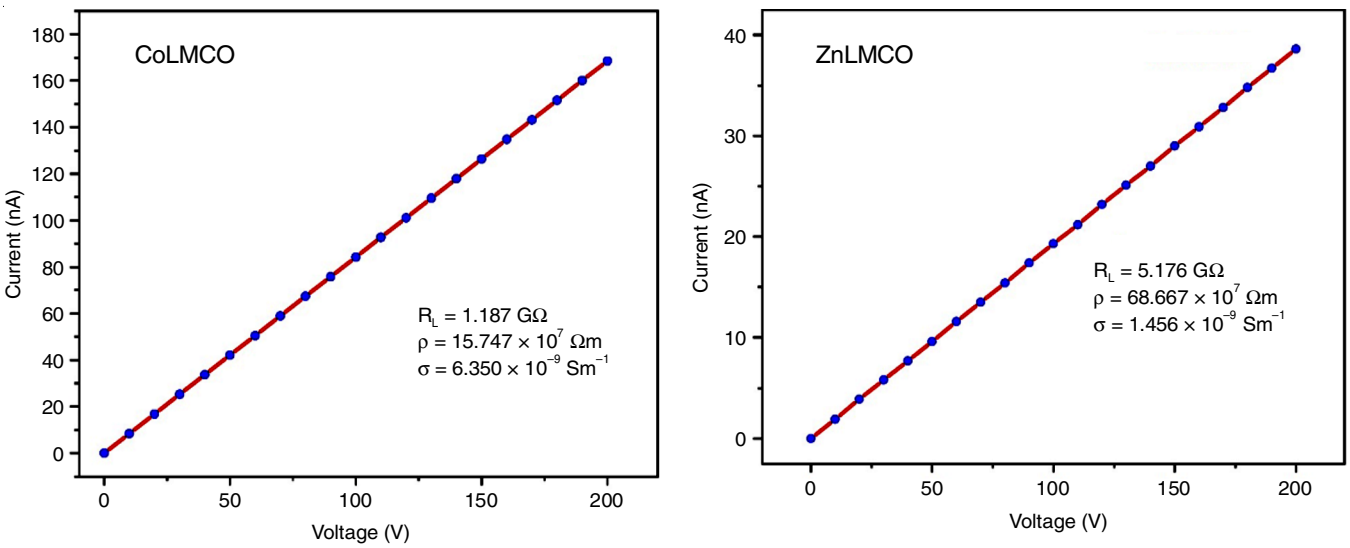

Fig. 9. V-I characteristics of CoLMCO and ZnLMCO crystals

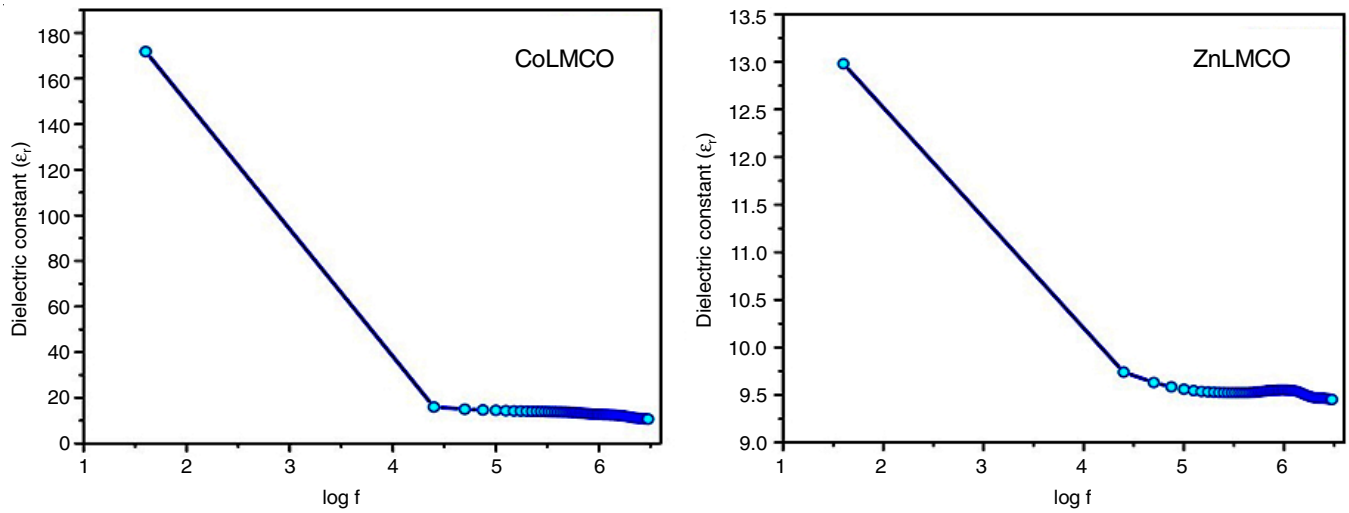

Fig. 10. Dielectric constant of CoLMCO and ZnLMCO crystals

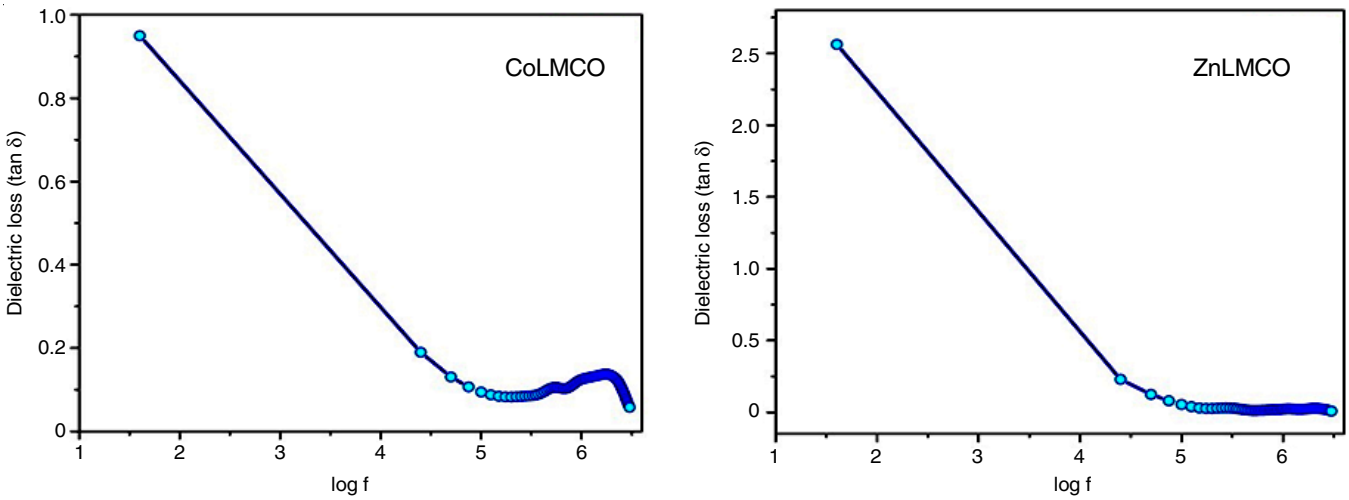

Fig. 11. Dielectric loss of CoLMCO and ZnLMCO crystals

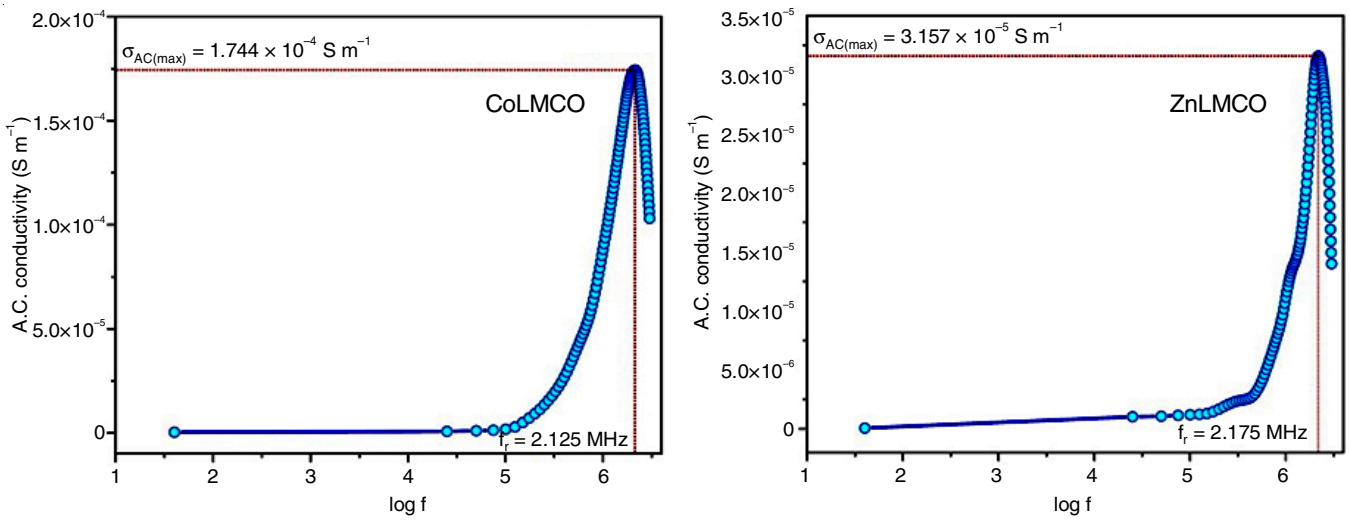

Fig. 12. AC conductivity of CoLMCO and ZnLMCO crystals

The opto-electrical and physical characteristics of crystalline CoLMCO and ZnLMCO compounds are intrinsically different. Since both the crystals exhibit high thermal stability in the metal oxide state, transmission in the visual spectrum, high refractive index and low reflectance; find their applications in developing opto-electronic devices. The prepared cadmium oxalate crystals due to their high leakage resistance (GΩ) and stable dielectric properties would provide good

electrical insulation in microelectronic applications such as gate insulation in MOSFET. The stability in dielectric behaviour with applied frequency in both CoLMCO and ZnLMCO crystals also could be used in generating radio frequency signals (MHz).

Conclusion

Newly grown high quality crystalline crystals *viz*. CoLMCO and ZnLMCO were fabricated using gel technique originated as the reaction product of extrinsic Co^{2+} and Zn^{2+} doping to lead mixed cadmium oxalate crystals, respectively. CoLMCO and ZnLMCO crystals characterized using EDX ingrained with the cationic distribution of 245: 4: 1 (Cd^{2+}:Pb^{2+}:Co^{2+}) and 59.25: 2.25: 1 (Cd^{2+}:Pb^{2+}:Zn^{2+}) respectively, which are in contrast to the cationic complex programmed in the growth phase (1:1:1). The presence of water of crystallization, oxalate group and metal-oxygen bonding in both crystals were identified by FTIR studies. Thermogravimetric analysis of the prepared crystals displayed two phases of decomposition and ensured high thermal stability until 1112.78 ºC in the Cd:Pb:Co-O state and up to 1071.65 ºC in the Cd:Pb:Zn-O state. The PXRD measurements of foresaid oxalate crystals revealed high crystallinity in the *P*1 space group, indicative of triclinic geometry. Both crystals showed absorption maxima in the UV region and complete transparency in the visible region; the ZnLMCO crystal exhibited comparatively high optical band gap energy (E_g = 5.845 eV), lower refractive index (n = 1.826) and reflectance (R = 0.085) than CoLMCO crystals (E_g = 5.638 eV, n = 1.862 and R = 0.091). The linear variation of current to applied voltage yielded a leakage resistance of 1.187 GΩ and DC conductivity 6.350 × 10^{-9} S m^{-1} in CoLMCO, whereas R_L = 5.176 GΩ and σ = 1.456 × 10^{-9} S m^{-1} for ZnLMCO crystals. The approach to stability in dielectric constant at higher frequencies and AC conductivity results of crystalline materials signal their implementation for resonance activities. Consequently, the superior thermal stability, transparency in the visible region, wide band gap energy, high leakage resistance and consistency in dielectric behaviour at higher frequencies indicate these crystalline crystals are instrumental as optical and electrical components in propelling technological advancements.

ACKNOWLEDGEMENTS

The authors are thankful to DST-PURSE laboratory, Mangalore University, Karnataka and STIC laboratory, Cochin University, Kerala, India for providing the research laboratory facilities.

CONFLICT OF INTEREST

The authors declare that there is no conflict of interests regarding the publication of this article.

REFERENCES

1. D.J. Price, A.K. Powell and P.T. Wood, *Dalton Trans*., 2478 (2003); https://doi.org/10.1039/B301658G
2. N. Jagannatha and P. Mohan Rao, *Bull. Mater. Sci.*, **16**, 365 (1993); https://doi.org/10.1007/BF02759549
3. M.M. Khunur, D.T. Wahyuni and Y.P. Prananto, *Adv. Nat. Appl. Sci.*, **5**, 467 (2011).
4. G. Marinescu, M. Andruh, F. Lloret and M. Julve, *Coord. Chem. Rev*., **255**, 161 (211); https://doi.org/10.1016/j.ccr.2010.08.004
5. N. Ponnappa, J. Nettar, H. Mylnahalli, D. D'Souza and L. Neratur, *Cryst. Res. Technol.*, **53**, 1700261 (2018); https://doi.org/10.1002/crat.201700261
6. D. Dollimore, *Thermochim. Acta*, **117**, 331 (1987); https://doi.org/10.1016/0040-6031(87)88127-3
7. https://www.nasa.gov/wp-content/uploads/2009/07/190387main_cosmic_elements.pdf
8. M. Iqbal, M. Muneer, R. Raza and M.A. Jamal, *Ceram. Int.*, **48**, 19681 (2022); https://doi.org/10.1016/j.ceramint.2022.03.105
9. K. Huang, J. Li and Z. Xu, *Waste Manag.*, **30**, 2292 (2010); https://doi.org/10.1016/j.wasman.2010.05.010
10. H.T. Kalmus, C.H. Harper and W.L. Savell, *Ind. Eng. Chem.*, **7**, 379 (1915); https://doi.org/10.1021/ie50077a004
11. M. Li and J. Lu, *Science*, **367**, 979 (2020); https://doi.org/10.1126/science.aba9168
12. http://metalpedia.asianmetal.com/metal/zinc/application.shtml
13. S.M.D. Prakash and P.M. Rao, *Bull. Mater. Sci.*, **8**, 511 (1986); https://doi.org/10.1007/BF02744117
14. P.S. Rohith, N. Jagannatha, K.V. Pradeepkumar, M.S. Mangala, K.P. Nagaraja and D. D'Souza, *Indian J. Pure Appl. Phys.*, **59**, 693 (2021).
15. F.D. Selasteen, S.A.C. Raj, A.A. Moses, F.E. Prince, R.E. Getsy and R. Elakkiya, *J. Cryst. Process. Technol.*, **6**, 11 (2016); https://doi.org/10.4236/jcpt.2016.62002
16. H.S. Pawar, S.J. Nandre, S.D. Chavhan and R.R. Ahire, *Int. J. Emerg. Technol. Innov. Res.*, **8**, 737 (2021).
17. M.R. Shedam, R.M. Shedam and S.N. Mathad, *Acta Chemica Iasi*, **25**, 195 (2017); https://doi.org/10.1515/achi-2017-0016
18. S. Sudha, C.R.T. Kumari, M. Nageshwari, P. Ramesh, G. Vinitha, M.L. Caroline, G. Mathubala and A. Manikandan, *J. Mater. Sci. Mater. Electron.*, **31**, 15028 (2020); https://doi.org/10.1007/s10854-020-04066-3
19. B.B. Parekh, P.M. Vyas, S.R. Vasant and M.J. Joshi, *Bull. Mater. Sci.*, **31**, 143 (2008); https://doi.org/10.1007/s12034-008-0025-1
20. P.S. Rohith, N. Jagannatha and K.V. Pradeep Kumar, *Bull. Mater. Sci.*, **44**, 185 (2021); https://doi.org/10.1007/s12034-021-02486-3
21. A.M. Ezhil Raj, D.D. Jayanthi and V.B. Jothy, *Solid State Sci.*, **10**, 557 (2008); https://doi.org/10.1016/j.solidstatesciences.2007.10.019
22. A. Altomare, G. Campi, C. Cuocci, L. Eriksson, C. Giacovazzo, A. Moliterni, R. Rizzi and P.-E. Werner, *J. Appl. Cryst*., **42**, 768 (2009); https://doi.org/10.1107/S0021889809025503
23. P. Vasudevan, S. Sankar and D. Jayaraman, *Bull. Korean Chem. Soc.*, **34**, 128 (2013); https://doi.org/10.5012/bkcs.2013.34.1.128
24. S. Ravi, S. Chenthamarai and R. Jayavel, *Int. J. Res. Eng. Technol.*, **4**, 457 (2015).
25. P.G. Jebaraj and V. Sivashankar, *Bulg. J. Phys.*, **50**, 127 (2023); https://doi.org/10.55318/bgjp.2023.50.2.127
26. D. D'Souza and K.P. Nagaraja, *Cryst. Res. Technol.*, **57**, 2100138 (2021); https://doi.org/10.1002/crat.202100138
27. P.S. Rohith, N. Jagannatha, K.V. Pradeepkumar and M.S. Mangala, *J. Phys. Conf. Ser.*, **1495**, 012005 (2020); https://doi.org/10.1088/1742-6596/1495/1/012005
28. R. Ramalakshmi, S. Stella Mary, S. Shahil Kirupavathy, S. Muthu and R. Thomas, *Heliyon*, **7**, e06527 (2021); https://doi.org/10.1016/j.heliyon.2021.e06527